

Design and development of stimulated Raman spectroscopy apparatus using a femtosecond laser system

Babita Mallick, Adithya Lakshmana, V. Radhalakshmi and Siva Umapathy*

Department of Inorganic and Physical Chemistry, Indian Institute of Science, Bangalore 560 012, India

We present the design and development of a stimulated Raman scattering (SRS) experimental set-up using a femtosecond laser system. The set-up involves the generation of (i) a picosecond (ps) narrow-bandwidth (5–20 cm⁻¹) Raman pump, and (ii) a femtosecond (fs) broadband continuum Raman probe pulse (800–1050 nm) providing the Stokes field, covering vibrations in the range 300–2500 cm⁻¹. When the two fields interact with the system simultaneously, gain features are observed on top of the probe beam at frequency corresponding to the characteristic molecular vibration frequency of the system. The ratio of the probe spectrum with and without the Raman pump provides a background-free gain spectrum. We present initial studies on some standard systems, viz. benzene, cyclohexane and β -carotene in CCl₄/benzene. These studies indicate that this technique provides a better signal with improved signal-to-noise ratio even for a low acquisition time in comparison with normal Raman spectroscopy.

Keywords: Design and development, laser system, optical pulses, stimulated Raman scattering.

RAMAN spectroscopy is a powerful, vibrational, structure-elucidating technique. It is widely used to understand the structure and dynamics of various photochemical and photophysical processes. However, it is a weak scattering phenomenon characterized by a low scattering cross-section (10⁻²⁹ cm²). Typically, out of million of photons, only one incident photon undergoes Raman scattering in propagating through 1 cm of scattering medium. Thus, one needs to accumulate for a longer time to obtain a better signal. Additionally, if a fluorescent molecule absorbs the incident photon, the intense fluorescence masks the weak Raman scattering. This makes it difficult to obtain any structural information for fluorescent molecules. Nevertheless, the weak Raman signal can be enhanced in resonance condition, where the incident photon has the same frequency as the characteristic absorption frequency of the molecule of interest. Under such conditions, one can achieve an enhancement of 10⁶, but at the expense of in-

creasing the background due to fluorescence. Since both fluorescence and Raman scattering are emitted isotropically (incoherently), normally the fluorescence cannot be suppressed easily. To overcome the fluorescence problem many techniques, such as coherent anti-Stokes Raman scattering (CARS)¹, picosecond optical Kerr-gate effect² and stimulated Raman scattering (SRS)³⁻⁵ have been developed. In this article, we discuss stimulated Raman spectroscopy that provides good enhancement of signal with an effective fluorescence rejection. Woodbury and Ng⁶ accidentally discovered SRS in 1962 using a Q-switched ruby laser with a nitrobenzene Kerr cell. Since then, it has been extensively used for the generation of coherent light sources, determination of vibrational lifetimes and as a vibrational pumping technique using continuous-wave, nanosecond and picosecond lasers^{3-5,7-9}. Recently, the advent of femtosecond lasers has made it possible to obtain a high peak power along with moderate average power in order to facilitate high efficiency collection of Raman-scattered light. In addition, the ease of generating broadband continuum using femtosecond lasers and its inherent fast time-resolution make it possible to study the dynamics of several ultrafast photochemical and photophysical processes. Thus, in recent years, the development of femtosecond stimulated Raman spectroscopy has become popular¹⁰⁻¹⁴. Here we discuss the design and development of our SRS experimental set-up using femtosecond laser system. First, we briefly present the principle of SRS followed by the experimental details. Next, we discuss the standardization of the SRS experimental set-up.

Principle of SRS

SRS is a third-order nonlinear ($\chi^{(3)}$) process that employs two optical pulses, viz. a Raman pump pulse (ω_p) and a Raman probe pulse (ω_s). When the two optical fields are simultaneously incident on a sample with molecular vibrational frequency (ω_v) equal to ($\omega_p - \omega_s$), attenuation of the Raman pump occurs and gain in Raman probe at a frequency corresponding to the difference between the Raman pump and molecular vibration (ω_v) is observed. This four-wave mixing process (SRS) can be understood by the use of the energy level diagram¹⁴, as illustrated in

*For correspondence. (e-mail: umapathy@ipc.iisc.ernet.in)

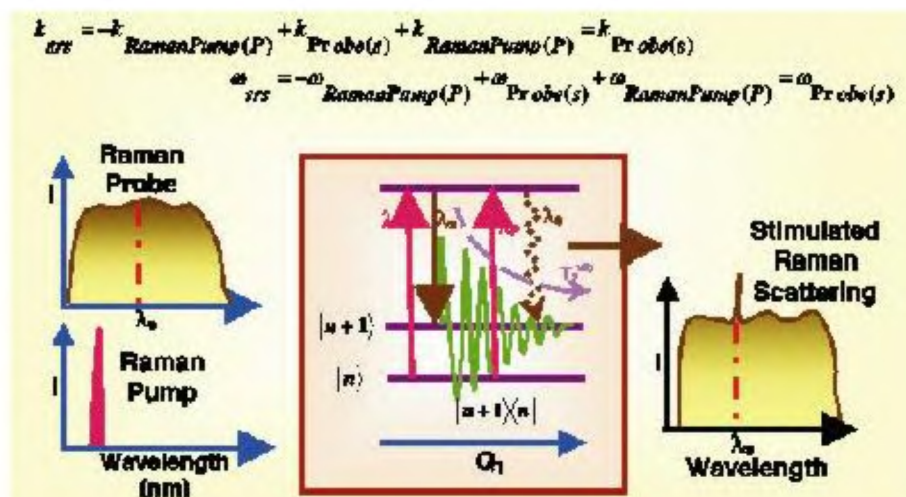


Figure 1. Stimulated Raman scattering (SRS). Raman pump (λ_p) and Raman probe (λ_s) on simultaneous interaction form a vibrational coherence ($|n+1\rangle\langle n|$), which decays with vibrational dephasing time (T_2^{vib}). During dephasing, another coupling of the Raman pump (λ_p) with the system occurs followed by subsequent emission of a photon (λ_s). SRS is a self-matched process ($k_{\text{srs}} = -k_{\text{Raman pump (p)}} + k_{\text{Probe (s)}} + k_{\text{Raman pump (p)}} = k_{\text{Probe (s)}}$).

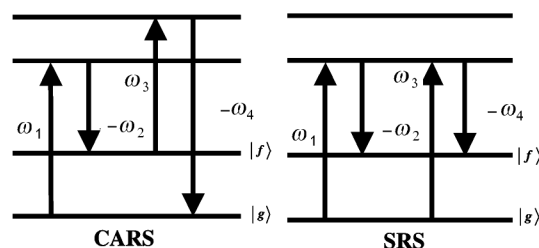
Figure 1. The Raman pump and Raman probe on simultaneous interaction with the system establish a vibrational coherence ($|n+1\rangle\langle n|$), which decays with the characteristic vibrational dephasing time (T_2^{vib}) of that particular mode of the system. During dephasing, another coupling of the Raman pump with the system occurs followed by the subsequent emission of a photon (ω_s). Importantly, SRS is a self-matched process ($k_{\text{srs}} = -k_{\text{Raman pump (p)}} + k_{\text{Probe (s)}} + k_{\text{Raman pump (p)}} = k_{\text{Probe (s)}}$), and results in the emission of a photon coherently with the probe beam thereby not affected by any spontaneous process (fluorescence). This is in distinct contrast with CARS, which requires specific three-pulse phase matching, thus making signal detection difficult. Figure 2 provides the energy-level diagram for SRS and CARS. Notably in SRS, it is the arrival of the Raman probe that initiates vibrational coherence which decays with beat frequency ($\propto 1/T_2^{\text{vib}}$) of the Raman pump and probe; and the convolution of the duration of the Raman pump and vibrational dephasing time determines the width of the signal¹⁴. In general, vibrational dephasing occurs in femtosecond timescale. Therefore, in case of a longer duration (picosecond) Raman pump, the pump solely decides the spectral width.

Theoretically, SRS can be understood using coupled wave equations, where the Raman pump and probe are coupled parametrically through the third-order nonlinear polarization ($P^{(3)}$) of the molecular system^{10,15–20}.

The differential scattering cross-section for SRS is given by:

$$\frac{d^2\sigma_{\text{SRS}}}{d\Omega d\omega_s} = \frac{32\pi^2 \hbar \omega_p \omega_s F(\omega_s)}{c^2 N} \text{Im} \chi_R^3, \quad (1)$$

where $F(\omega_s)$ is the spectral photon flux (photons $\text{cm}^{-2} \text{s}^{-1} \text{Hz}^{-1}$), and N the number of molecules per unit volume.



In CARS

$\omega_1 = \omega_3 = \omega_{\text{pump}}$ and $\omega_2 = \omega_{\text{probe}}$.
phase matching condition is $2k_1 - k_2 = k_4$.

In SRS

$\omega_1 = \omega_3 = \omega_{\text{pump}}$ and $\omega_2 = \omega_{\text{probe}}$.
phase matching condition is $k_1 - k_2 - k_1 = -k_4$.

Figure 2. Illustration of coherent anti-Stokes Raman scattering and SRS energy-level diagram.

The spontaneous differential Raman cross-section is:

$$\frac{d^2\sigma_{\text{Spont}}}{d\Omega d\omega_s} = \frac{\hbar \omega_p \omega_s^3}{\pi c^4 N} \text{Im} \chi_R^3. \quad (2)$$

Thus, the ratio of the two differential scattering cross-sections obtained is:

$$\frac{d^2\sigma_{\text{SRS}}}{d^2\sigma_{\text{Spont}}} = \frac{32\pi^3 c^2}{\omega_s^2} F(\omega_s). \quad (3)$$

Equation (3) indicates that the gain increases with increase in flux of the Raman probe and as Stokes frequency shifts to red where the zero-point radiation density-of-states decreases. Moreover, since it is a self-phase matched

and a coherent process, spontaneous processes do not affect it. Hence, fluorescent molecules can be studied using SRS, unlike in spontaneous Raman scattering. Another important aspect of SRS is that since in this process the gain observed in the probe is proportional to the imaginary part (resonant) of the nonlinear susceptibility (eq. (1)), the spectral shape is closely related to spontaneous spectroscopy. Unlike SRS, in CARS the signal intensity depends also on the real part (non-resonant) of nonlinear susceptibility that distorts the signal¹⁸.

The above-mentioned characteristics of SRS can be used to understand the time-dependent dynamics of various systems, as explained here. In time-resolved SRS, a femtosecond (fs) pulse (λ_{exc}) is used to generate the excited state, which is then probed by SRS. For SRS, a picosecond (ps) near-infrared (NIR) pulse is used as the Raman pump pulse, while the Raman probe is a fs broadband continuum providing the Stokes field with respect to the Raman pump. As we know, in SRS the signal photons can be emitted at any time during vibrational dephasing. Nonetheless, the initiation of the vibration coherence depends on the arrival of the Raman probe beam, which can be resolved with fs precision with respect to the fs λ_{exc} pulse. Therefore, the temporal resolution depends on the cross-correlation between the fs λ_{exc} pulse forming the excited state and the Raman probe initiating the coherence. However, convolution of the Raman pump and the vibrational dephasing time determine the spectral resolution. Hence, in SRS, the spectral resolution and the temporal resolution are deconvoluted, unlike in conventional fs time-resolved Raman studies (pump-probe). In the pump-probe technique, the temporal and spectral resolutions are dependent on each other owing to the energy-time uncertainty principle. Thus, in these studies the spectral resolution is poor even though the temporal resolution is in fs.

These above-mentioned advantages make SRS a unique structure-elucidating tool. Here we report studies on ben-

zene, cyclohexane and β -carotene used to standardize the SRS system.

Experimental details

Our SRS system employs the generation of two NIR pulses: a ps narrow bandwidth ($5\text{--}20\text{ cm}^{-1}$) Raman pump pulse centred at 787 nm, and a fs broadband continuum Raman probe pulse (800–1050 nm) providing the Stokes field covering vibrations in the range $300\text{--}2500\text{ cm}^{-1}$, from a 105 fs laser source. When the two fields overlap spatially and temporally on the sample, one observes gain features on top of the probe beam. The ratio of the probe spectrum for the Raman pump on and off, gives the gain spectrum (Figure 3). Use of a long duration ps pulse as Raman pump ensures a good spectral resolution.

Laser system

The stimulated Raman laser set-up (Figure 4) consists of a Ti:sapphire regenerative amplifier (Spitfire, Spectra Physics) seeded by mode-locked Ti:sapphire laser (110 fs, 8.75 nJ, 80 MHz, Tsunami, Spectra Physics). The Ti:sapphire regenerative amplifier amplifies the seed laser by chirped pulse amplification and generates a 105 fs pulse at a repetition rate of 1 kHz and having a pulse energy of 2.2 mJ centred at 788 nm. A 50:50 beam-splitter splits the amplifier output into two halves. One half was used to produce the Raman pump, while the other was used for the Raman probe, as described below.

Raman pump

The Raman pump was generated by spectrally filtering a portion of the amplifier output using home-designed spectral filter. The spectral filter consists of two gratings

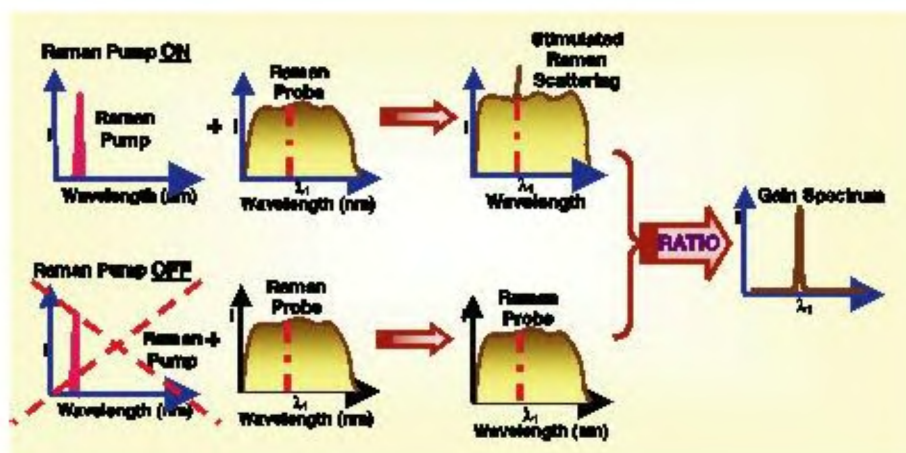


Figure 3. Gain spectrum. The ratio of the probe spectrum with and without the Raman pump gives the gain spectrum. SRS occurs only when both beams are present. Gain = (Raman probe with Raman pump on)/(Raman probe with Raman pump off).

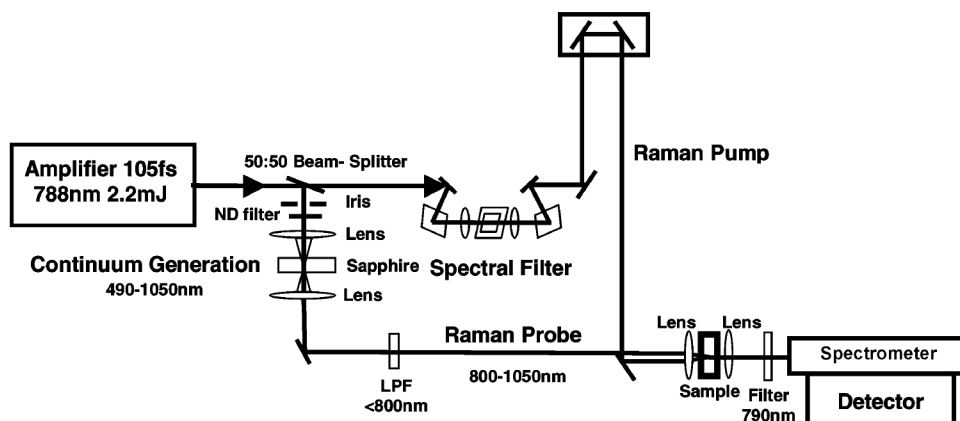


Figure 4. SRS experimental set-up.

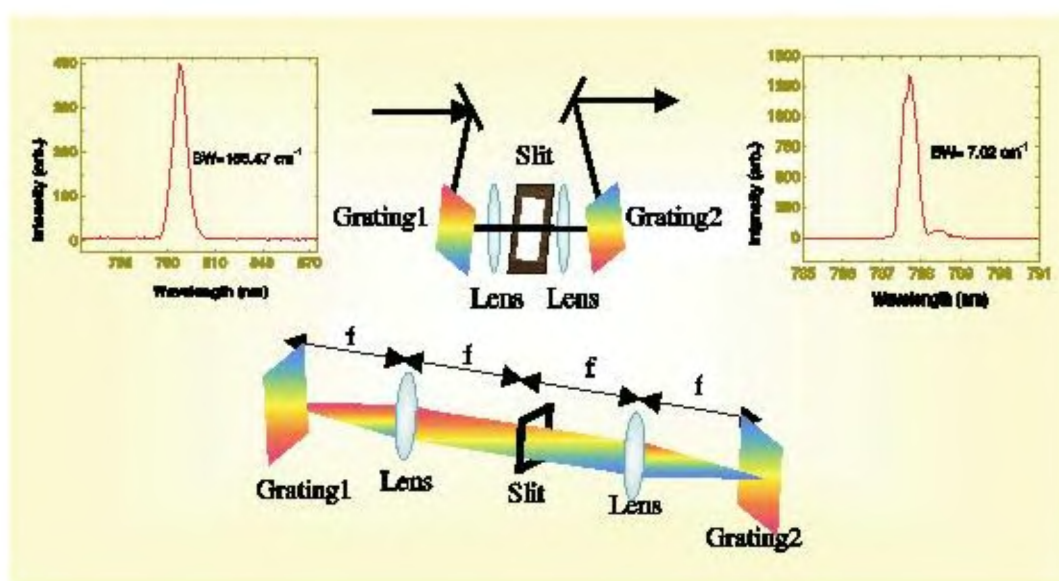


Figure 5. Spectral filter. Raman pump generated: Energy = 1.02 μJ ; $\lambda_{\text{central}} = 787.712 \text{ nm}$; bandwidth = 7.02 cm^{-1} ; integration time (IT) = 100 ms; spectrometer slit = 200 μm .

(1200 g/mm, 750 nm blaze), an adjustable slit and two lenses of 150 mm focal length. Figure 5 depicts the arrangement of each of the components^{21,22}. The distance between each component is equal to the focal length of the lens. This arrangement reduces the angular dispersion as well as the group velocity dispersion of the beam. After the 50 : 50 beamsplitter, the amplifier output was attenuated by an aperture to a beam of size 5 mm and energy 200 μJ , and incident on the first grating, which in turn disperses the beam in spectral domain. The first 150 mm focal length lens focused the dispersed beam on the slit. The width of the slit determines the bandwidth, while its lateral position decides the central wavelength of the Raman pump. Then, the second lens (150 mm fl) collimated the beam and the second grating removed the dispersion. We were able to produce Raman pump having 2–4 μJ of energy centred at 787 nm with a bandwidth of 5–20 cm^{-1} .

Raman probe

The amplifier output was attenuated to a beam of size 3 mm and energy 1 μJ using an iris and neutral density filter. The beam was focused onto a 2 mm sapphire crystal generating a stable continuum. A stable continuum was produced by adjusting the power of the incident beam using a combination of iris and neutral density filter and the focal point at sapphire. The continuum generated ranged from 490 to 1050 nm. A long wave pass filter (10LWF950) was used to allow only the Stokes region with respect to Raman pump of the continuum generated (Figure 6).

Data collection

Both the beams were made to travel parallel to each other. Then, a single lens of focal length 75.6 mm was

used to focus the two beams onto the sample. The beam diameters of the Raman pump and probe at sample were 25.264 and 16.950 μm respectively. The Raman probe containing SRS was collected using a lens (50.8 mm) and focussed onto a spectrograph (TRIAx 550, 1200 g/mm, 750 nm blaze) connected with a LN_2 cooled CCD detector. A sharp cut-off filter (RG830) was placed on the probe path before the spectrometer to cut the Raman pump and Rayleigh scattering (Figure 4).

The probe spectrum was collected for different delays between the Raman pump and probe. In addition, at each delay the probe spectrum with Raman pump on and off was taken. Gain features on top of the probe were observed as the two beams overlapped in time with maximum signal appearing at time delay equal to zero. The gain appeared at the characteristic vibrational frequency of the sample. The gain is given by:

$$\text{Gain} = \frac{\text{Raman probe with Raman pump on}}{\text{Raman probe with Raman pump off}}$$

Results and discussion

We have used the stimulated Raman spectrometer described above to record the SRS spectrum of benzene,

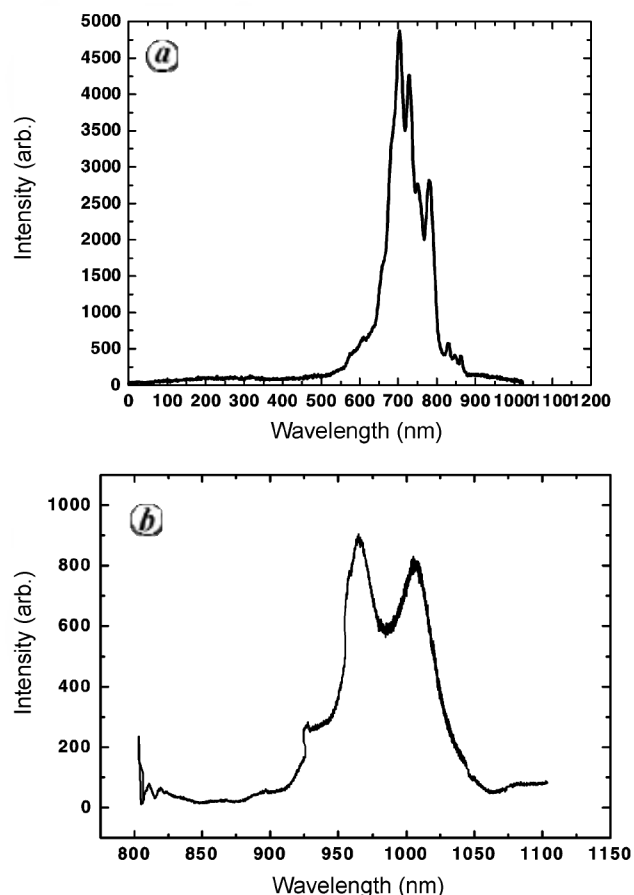


Figure 6. Raman probe spectrum without (a) and with (b) the long wave pass filter (10LWF950).

cyclohexane and β -carotene (in CCl_4 and benzene). β -Carotene was chosen as it is a well-studied system and its vibrational frequencies are well documented in the literature²³.

SRS of cyclohexane

Stimulated Raman spectrum of cyclohexane (AR, Sigma-Aldrich) was recorded using a cuvette of 1 mm path-length. The characteristics of the Raman pump used were λ_{central} , 787.78 nm; bandwidth, 17.54 cm^{-1} ; energy, 1.25 μJ , and beam diameter at the sample point, 24.7 μm . The probe energy used was 0.62–0.43 nJ. The beam diameter of the probe at the sample point was 12.5 μm . The characteristic cyclohexane peaks at 801.4 cm^{-1} (C–C str), 1029.2 cm^{-1} (C–C str), 1156 cm^{-1} (CH_2 rock), 1265.2 cm^{-1} (CH_2 twist) and 1442.5 cm^{-1} (CH_2 scissor) were observed^{16,24}. Figure 7a depicts the Raman probe spectrum with Raman pump on and off. The ratio of the two gives the gain spectrum (Figure 7b). The SRS spectrum at different spectral windows (1355 and 925 cm^{-1}) was compared with the corresponding spontaneous Raman spectrum (Figure 8). In case of the peak at 1265.2 cm^{-1} , the SRS signal was 19 times the count observed for spontaneous Raman, while the peak at 801.4 cm^{-1} was enhanced 11 times. Figure 9 shows the SRS spectrum of cyclohexane as a function of the delay between the Raman pump and the probe. The maximum signal appeared at zero delay, i.e. when there was a maximum temporal overlap between the two beams. As the delay was varied ± 800 fs with respect to the zero delay, the gain decreased.

SRS of benzene

The stimulated Raman spectrum of benzene (AR, Sigma-Aldrich) was recorded. The Raman pump used was centred at 787.712 nm, with a bandwidth of 7.02 cm^{-1} . The Raman pump energy and beam diameter at the sample point were 1.02 μJ and 25.2 μm respectively. The probe energy and beam diameter were 0.37 nJ @880 nm and 16.9 μm respectively. Figure 10 shows the Raman spectrum of benzene obtained by SRS and spontaneous Raman scattering. We observed that the 993 cm^{-1} peak corresponding to C=C ring stretching¹⁶ of benzene was enhanced 100 times by SRS compared to normal Raman scattering.

SRS of β -carotene

The stimulated Raman spectrum of 10^{-2} M solution of β -carotene in CCl_4 and benzene was recorded. β -Carotene (Sigma-Aldrich) was used as received. The characteristics of the Raman pump used for SRS of β -carotene in CCl_4 were λ_{central} , 787.711 nm; bandwidth, 6.51 cm^{-1} ; energy, 0.99 μJ , and beam diameter at the sample point, 24.7 μm .

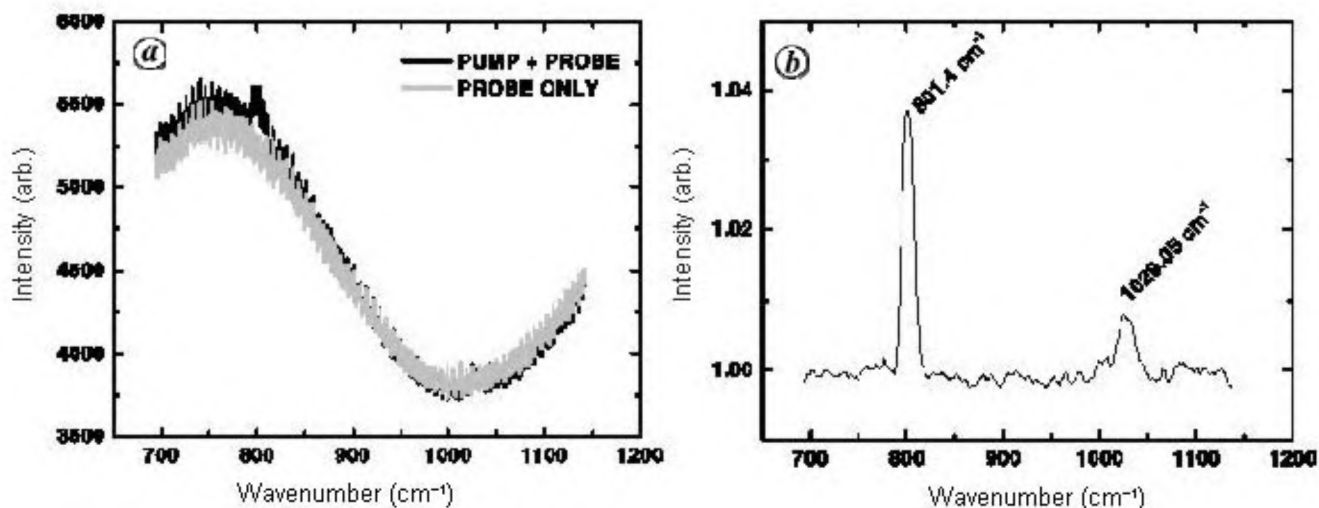


Figure 7. SRS spectrum of cyclohexane (IT = 2 s, accumulation = 10, slit = 150 μm). *a*, Raman pump + Raman probe, and only probe. *b*, Gain spectrum [(Raman pump + Raman probe)/(only probe)].

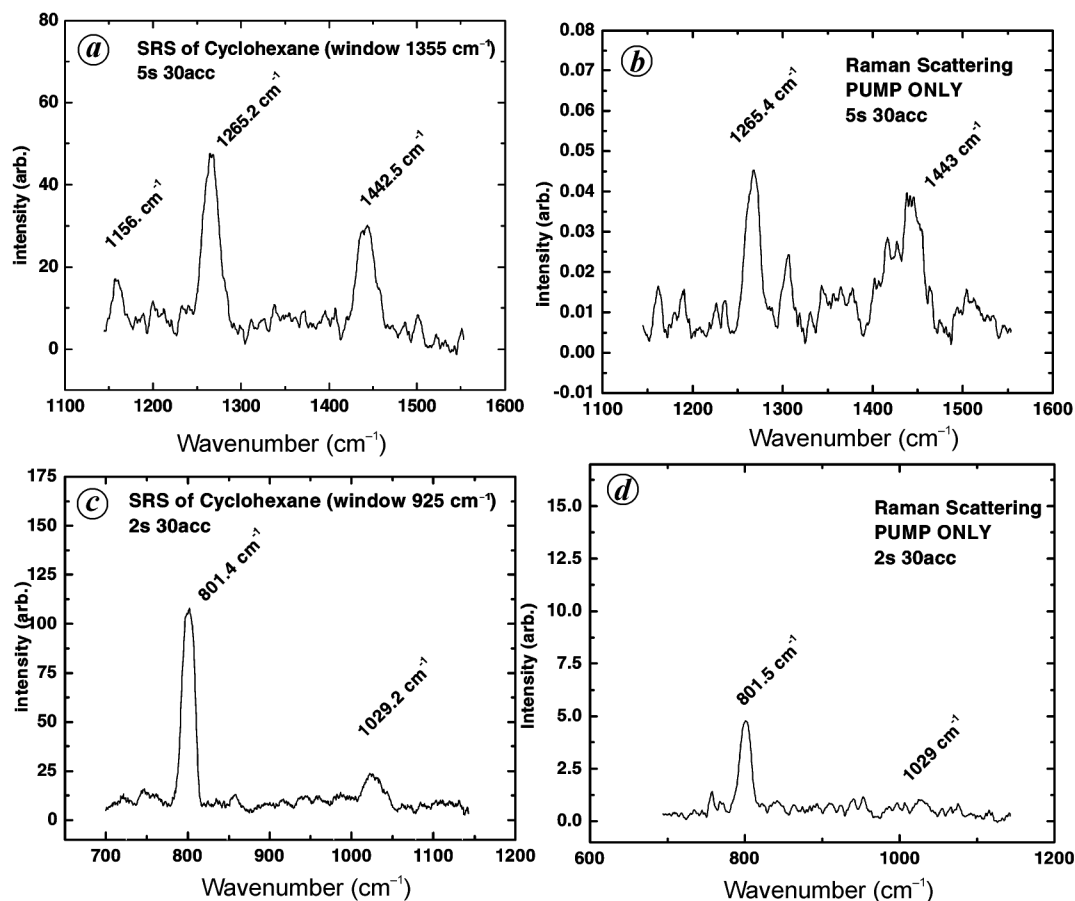


Figure 8. Comparison between spontaneous Raman and SRS spectra of cyclohexane. Pump $\rightarrow \lambda_{\text{central}}$ at 787.78 nm, BW = 17.54 cm⁻¹, energy = 1.25 μJ , beam diameter = 24.7 μm . *a*, *b*, Probe \rightarrow energy = 0.43 nJ @880 nm, beam diameter = 12.5 μm . *c*, *d*, Probe \rightarrow energy = 0.62 nJ @880 nm, beam diameter = 12.5 μm .

The probe energy used was 0.01 nJ. The beam diameter of the probe at the sample point was 16.9 μm . The characteristic 1528 cm⁻¹ (C=C str) and 1160.2 cm⁻¹ (C-C str)

peaks were observed (Figure 11*a*). The signal was observed even for a low integration time of 30 s, while for the same time normal Raman scattering was not observed

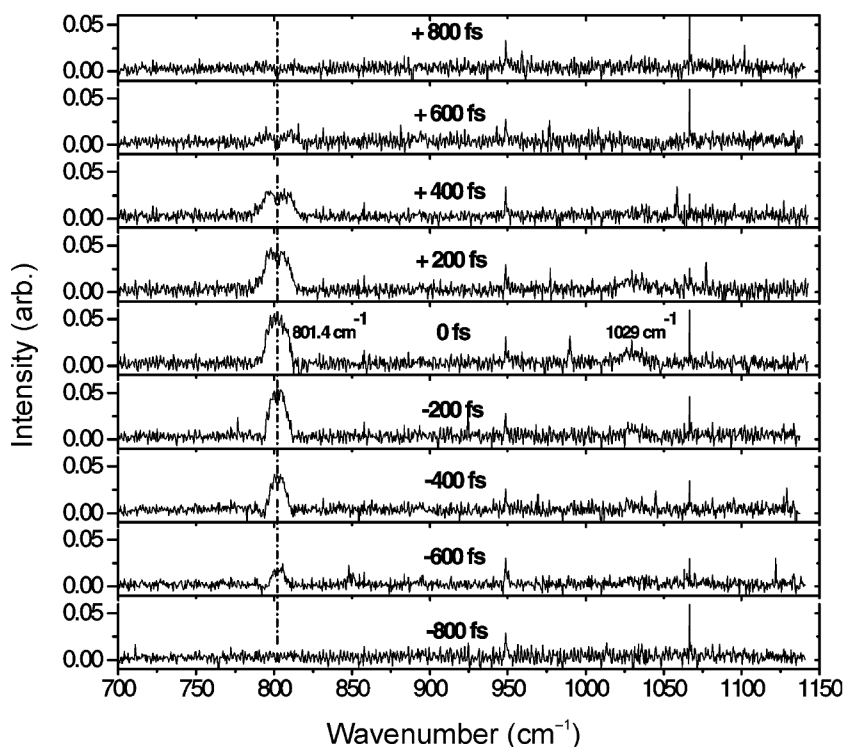


Figure 9. SRS spectrum of cyclohexane as a function of the delay between Raman pump and Raman probe.

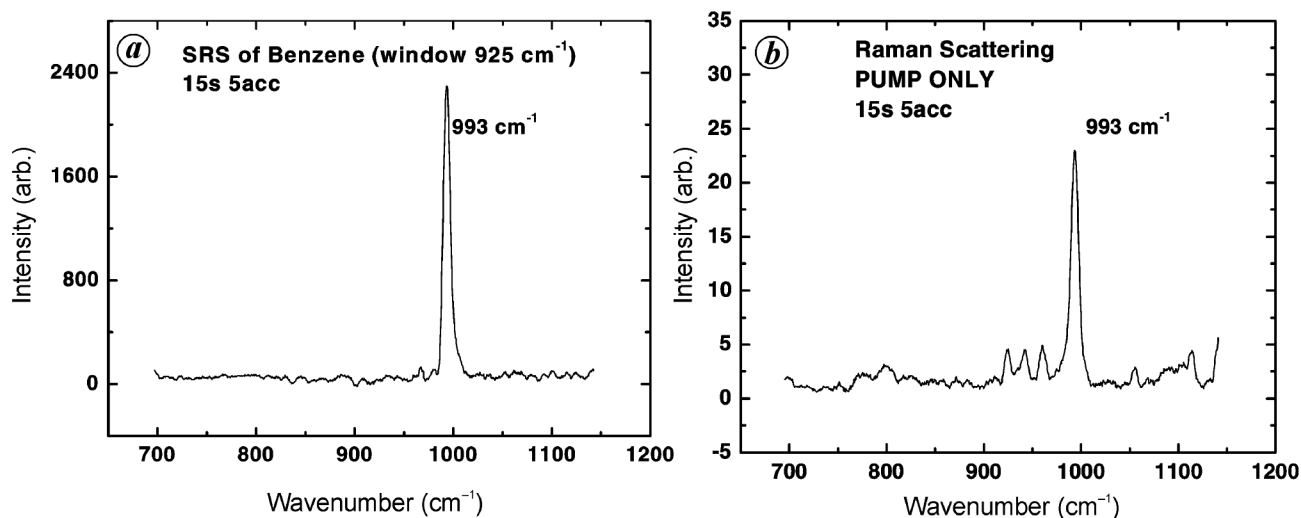


Figure 10. Comparison between SRS (a) and spontaneous Raman spectra (b) of benzene. Pump $\rightarrow \lambda_{\text{central}}$ at 787.712 nm, BW = 7.02 cm^{-1} , energy = 1.02 μJ , beam diameter = 25.2 μm . Probe \rightarrow energy = 0.37 nJ @880 nm, beam diameter = 16.9 μm .

(Figure 11 b). This indicates the advantage of low acquisition time required for SRS over normal Raman scattering.

For recording the SRS of β -carotene in benzene, the Raman pump used was centred at 787.697 nm, with a bandwidth of 7.05 cm^{-1} . The pump energy and beam diameter were 0.99 μJ and 25.2 μm respectively. The probe energy and beam diameter were 0.42 nJ @880 nm and 16.9 μm respectively. The 1528 cm^{-1} ($\nu_{\text{C}=\text{C}}$) and 1160.2 cm^{-1} ($\nu_{\text{C}-\text{C}}$) peaks were observed (Figure 12). In

case of SRS, there was almost 100-fold enhancement of the signal compared to the normal Raman spectrum (Figure 12).

Summary

We have developed a stimulated Raman spectrometer. Our system consists of two NIR beams used as Raman pump and Raman probe. The probe used is a continuum

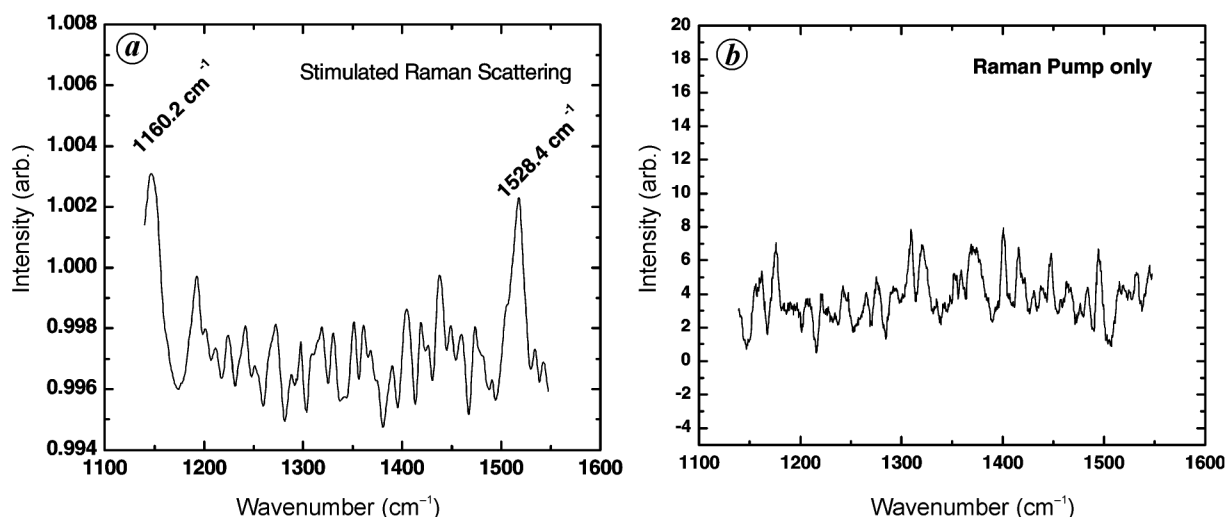


Figure 11. (a) SRS and (b) spontaneous Raman spectra of β -carotene in CCl_4 (IT = 30 s, accumulation = 5, slit = 200 μm). Pump $\rightarrow \lambda_{\text{central}}$ at 787.711 nm, BW = 6.51 cm^{-1} , energy = 0.99 μJ , beam diameter = 25.2 μm . Probe \rightarrow energy = 0.01 nJ @880 nm, beam diameter = 16.9 μm .

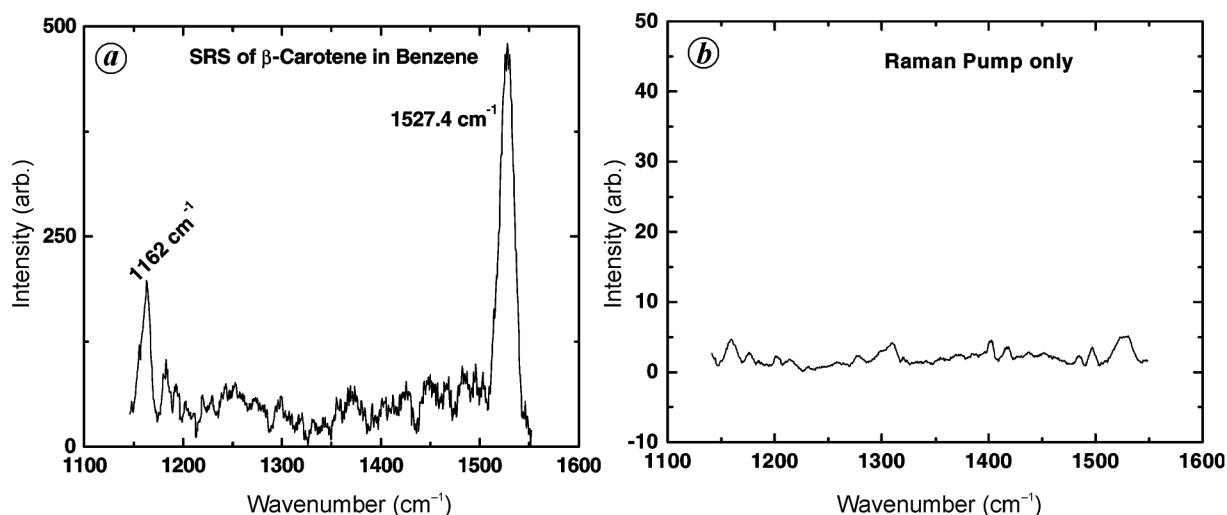


Figure 12. (a) SRS and (b) spontaneous Raman spectra of β -carotene in benzene (IT = 20 s, accumulation = 10, slit = 200 μm). Pump $\rightarrow \lambda_{\text{central}}$ at 787.697 nm, BW = 7.05 cm^{-1} , energy = 0.99 μJ , beam diameter = 25.2 μm . Probe \rightarrow energy = 0.42 nJ @880 nm, beam diameter = 16.9 μm .

covering Stokes region of Raman scattering, while the Raman pump is a narrow bandwidth (5–20 cm^{-1}) ps pulse centred at 787 nm. Initial studies were carried out using some standard systems, viz. benzene, cyclohexane and β -carotene in CCl_4 /benzene. The initial results indicate that SRS leads to better signal for low acquisition time and a better signal-to-noise ratio in comparison with normal Raman spectroscopy.

1. Begley, R. F., Harvey, A. B. and Byer, R. L., Coherent anti-Stokes Raman spectroscopy. *Appl. Phys. Lett.*, 1974, **25**, 387–390.
2. Matousek, P., Towrie, M., Stanley, A. and Parker, A. W., Efficient rejection of fluorescence from Raman spectra using picosecond Kerr gating. *Appl. Spectrosc.*, 1999, **53**, 1485–1655.
3. Owyong, A., Coherent Raman gain spectroscopy using CW laser sources. *IEEE J. Quantum Electron.*, 1978, **14**, 192–203.

4. Werneke, W., Lau, A., Pfeiffer, M., Weigmann, H.-J., Hunsalz, G. and Lenz, K., Inverse resonance Raman scattering and resonance Raman amplification. *Opt. Commun.*, 1976, **16**, 128–132.
5. Wong, K. H., Ho, W. L. and Tsui, W. L., Stimulated Raman gain spectroscopy seeded by amplified spontaneous emission. *J. Raman Spectrosc.*, 1992, **23**, 479–481.
6. Woodbury, E. J. and Ng, W. K., Ruby laser operation in the Near IR. *Proc. IRE*, 1962, **50**, 2367.
7. Laubereau, A. and Kaiser, W., Vibrational dynamics of liquids and solids investigated by picosecond light pulses. *Rev. Mod. Phys.*, 1978, **50**, 607–665.
8. Laubereau, A., von der Linde, D. and Kaiser, W., Direct measurements of the vibrational lifetimes of molecules in liquids. *Phys. Rev. Lett.*, 1972, **28**, 1162–1165.
9. Esherrick, P. and Owyong, A., High resolution stimulated Raman spectroscopy. In *Advances in Infrared and Raman Spectroscopy* (eds Clark, R. J. H. and Hester, R. E.), Wiley Heyden, London, 1982, vol. 9, pp. 130–187.

10. McCamant, D. W., Kukura, P. and Mathies, R. A., Femtosecond broadband stimulated Raman: a new approach for high-performance vibrational spectroscopy. *Appl. Spectrosc.*, 2003, **57**, 1317–1323.
11. Yoshizawa, M. and Kurosawa, M., Femtosecond time-resolved Raman spectroscopy using stimulated Raman scattering. *Phys. Rev. A*, 1999, **61**, 013808-1–013808-6.
12. Jin, S. M., Lee, Y. J., Ku, J. and Kim, S. K., Development of femtosecond stimulated Raman spectroscopy: stimulated Raman gain via elimination of cross phase modulation. *Bull. Korean Chem. Soc.*, 2004, **25**, 1829–1832.
13. Laimgruber, S., Schachenmayr, H., Schmidt, B., Zinth, W. and Gilch, P., A femtosecond stimulated Raman spectrograph for the near ultraviolet. *Appl. Phys. B*, 2006, **85**, 557–564.
14. Kukura, P., McCamant, D. W. and Mathies, R. A., Femtosecond stimulated Raman spectroscopy. *Annu. Rev. Phys. Chem.*, 2007, **58**, 461–488.
15. Shen, Y. R. and Bloembergen, N., Theory of stimulated Brillouin and Raman scattering. *Phys. Rev.*, 1965, **137**, A1787–A1805.
16. Bloembergen, N., The stimulated Raman effect. *Am. J. Phys.*, 1967, **35**, 989–1023.
17. Colles, M. J. and Griffiths, J. E., Relative and absolute Raman scattering cross sections in liquids. *J. Chem. Phys.*, 1972, **56**, 3384–3391.
18. Penzkofer, A., Laubereau, A. and Kaiser, W., High intensity Raman interactions. *Prog. Quantum Electron.*, 1979, **6**, 55–140.
19. Lee, D. and Albrecht, A. C., A unified view of Raman, resonance Raman, and fluorescence spectroscopy (and their analogues in two-photon absorption). In *Advances in Infrared and Raman Spectroscopy*, Wiley Heyden, London, 1985, vol. 12, pp. 179–213.
20. Soo-Y Lee, Zhang, D., McCamant, D. W., Kukura, P., and Mathies, R. A., Theory of femtosecond stimulated Raman spectroscopy. *J. Chem. Phys.*, 2004, **121**, 3632–3642.
21. Martinez, O. E., Gordon, J. P. and Fork, R. L., Negative group velocity dispersion using refraction. *J. Opt. Soc. Am.*, 1984, **1**, 1003–1006.
22. Martinez, O. E., 3000 Times grating compressor with positive group velocity dispersion: application to fiber compensation in 1.3–1.6 μm region. *IEEE J. Quantum Electron.*, 1987, **23**, 59–64.
23. Polivka, T. and Sundstrom, V., Ultrafast dynamics of carotenoid excited states – from solution to natural and artificial systems. *Chem. Rev.*, 2004, **104**, 2021–2071.
24. Takashi, Hiroaki and Shimanouchi, Takehiko, Infrared spectrum and normal vibrations of cyclohexane. *J. Mol. Spectrosc.*, 1964, **13**, 43–53.

ACKNOWLEDGEMENTS. We thank Indian Institute of Science, Bangalore and the Department of Science and Technology, New Delhi for funding this project. B.M. and A.L. thank CSIR, New Delhi for providing research fellowships.

Received 25 June 2008; revised accepted 10 November 2008

MEETINGS/SYMPOSIA/SEMINARS

5th International Conference on Biopesticides: Stakeholders' Perspectives

Date: 26–30 April 2009
Place: New Delhi, India

Themes include: Crops pest management: Microbial biopesticides; Botanical pesticides; Semio-chemicals; Parasitoids and predators. Pests of public health importance: Vector control; Household pests; Veterinary pests; Weed control. Novel approaches: Genomics, proteomics, and metabolomics; Nanotechnology and delivery systems; Strategies in integrated pest management (IPM). Laboratory to land issues: Research trends; Empowering farm women; Role of NGOs; Implementation strategies. Linking the stakeholders. Farmer's perspective; Policy and regulatory issues; Commercialization of biopesticides; Public-private partnership.

Contact: The Secretariat
5th International Conference on Biopesticides
The Energy and Resources Institute
Darbari Seth Block, IHC Complex
Lodhi Road
New Delhi 110 003, India
Tel: +91 11 2468 2100 or 4150 4900
Fax: +91 11 2468 2144 or 2468 2145
E-mail: icob2.biopest@nic.in
Website: www.icob5.nic.in

National Seminar on Recent Advances in Microbiology, Genetics and Biotechnology Research – 2009

Date: 20–22 January 2009
Place: Sivakasi

Topics include: Microbiology, Biotechnology, Proteomics, Genetics, Plant Breeding, Biodiversity, Immunology, Bioinformatics and Nanotechnology.

Contact: Dr D. Prabhu
Head and Organizing Secretary
Department of Microbiology and Genetics
Ayya Nadar Janaki Ammal College
Sivakasi 626 124
Tel: 04562 254100
Fax: 04562 254970
Mobile: 94421 87090
E-mail: anjaemicrobiology@yahoo.com
Website: www.anjac.org